Fuel 140 (2015) 744–751

Contents lists available at ScienceDirect

Fuel

journal homepage: www.elsevier.com/locate/fuel

Fast characterization of biomass fuels by thermogravimetric analysis (TGA)

Juan F. Saldarriaga, Roberto Aguado *, Aitor Pablos, Maider Amutio, Martin Olazar, Javier Bilbao

Department of Chemical Engineering, University of the Basque Country UPV/EHU, PO Box 644, E48080 Bilbao, Spain

HIGHLIGHTS

- A methodology for the full characterization of lignocellulosic biomass is proposed.
- Suitable TGA analysis allows an accurate determination of the proximate analysis.
- The DTG curve is used for the determination of the content of the natural polymers.
- Empirical correlations are obtained for predicting HHV and C, H and O contents.

ARTICLE INFO

Article history:
Received 29 April 2014
Received in revised form 10 October 2014
Accepted 13 October 2014
Available online 23 October 2014

Keywords:
Biomass
Elemental analysis
Proximate analysis
HHV
Thermogravimetry

ABSTRACT

A methodology is proposed based on thermogravimetric analysis, deconvolution of the DTG signal and empirical correlations for characterizing biomass fuels for boilers and combustors. This methodology allows determining accurately and in a short time the main parameters required for industrial operation, as are the higher heating value (HHV), the contents of moisture, volatile matter, fixed carbon, ashes, carbon, hydrogen and oxygen, and the kinetic parameters of the thermal decomposition of the biomass. At the present time, these parameters are obtained by using specific equipment that are much more sophisticated and expensive than the methodology proposed. Twelve types of vegetable lignocellulosic biomasses have been used in the study, i.e., wastes from wood industry, food industry and agriculture. The comparison of the results obtained, based on the methodology developed in this paper, with those published in the literature evidence the validity of the methodology for a wide range of materials.

© 2014 Elsevier Ltd. All rights reserved.

1. Introduction

Vegetable biomass is one of the oldest energy sources on which mankind supported development. Biomass was set aside in the XX century due to the increase in energy demand, especially in the developed countries, and to the availability and higher energy density of coal, natural gas, oil and their derivatives. Nevertheless, the limited availability of fossil resources and their location at given zones in the world create a great dependence on oil importing countries, which seriously affects energy supply and even the economy of the region. Furthermore, there is an increasing concern about the impact production processes, especially those for energy production, have on the environment, which makes unsustainable an energy system massively based on fossil fuels.

Bearing in mind the present scenario on which development and welfare are related to energy consumption, alternative energy production resources should be considered, especially those that are geographically well distributed, renewable and environmentally friendly by contributing to neutral CO_2 balance. Vegetable biomass fulfils these three conditions, and therefore increasing interest is being paid to this alternative and renewable source for energy and raw materials [1,2]. Thus, except in the extreme regions (polar icecaps and extremely dried zones), vegetal biomass grows around the world in different forms (herbaceous plants, bushes, trees, algae and so on). Furthermore, the development in agriculture techniques has greatly increased soil fertility, which has given way to the abandonment of agricultural land over the last 20–30 years. Sustainable use of this land for the production of crops for energy production is a reasonable option to decrease energy dependence and contribute to avoiding environmental deterioration.

The use of edible crops for energy production has arisen a great controversy for the last years due to the increase in the price of human food this practice causes [3], and therefore certain first generation biofuels (mainly oil and ethanol) have not reached the

---

* Corresponding author. Tel.:+34 946 015 394; fax: +34 946 013 500.
E-mail address: roberto.aguado@ehu.es (R. Aguado).

http://dx.doi.org/10.1016/j.fuel.2014.10.024
0016-2361/© 2014 Elsevier Ltd. All rights reserved.

Nomenclature

ASRE	average square relative error
c_i	mass concentration of i component (wt.%)
E_i	activation energy of i constituent (kJ mol^{-1})
k_i	kinetic constant for the weight loss of each i constituent (s^{-1})
$k_{i,ref}$	kinetic constant for the weight loss of each i constituent at the reference temperature (s^{-1})
N	number of experimental data
t	time (min)
W, W_0, W_∞	weight of biomass sample at t time, at the beginning of pyrolysis and at the end of pyrolysis, respectively (mg)
W_i, $W_{0,i}$, $W_{\infty,i}$	weight of i constituent in the sample at t time, at the beginning and at the end (mg)
X	conversion of the biomass sample by mass unit of pyrolysable mass
X_i, $X_{\infty,i}$	conversion of i constituent at t time and at the end

development expected. Nevertheless, this is not the case for lignocellulosic biomass, given that it cannot be digested by human beings and is composed of a wide range of materials, as are: wood, wood-derived products, energy crops, agricultural products, agricultural industry products, forest wastes, wood manufacturing wastes and so on [4].

The more developed technologies for obtaining energy or fuels from biomass are those based on thermochemical treatments, namely, pyrolysis, gasification and combustion. Although pyrolysis is a route of great interest from an industrial and ecological perspective [5] due to the high yield of bio-oil obtained [6,7], the high content of oxygen and the presence of phenolic oligomers are obstacles in which intensive research is being carried out in order to progress in the development of the biorefinery [8]. Gasification has been intensively developed over the last century and nowadays is considered a suitable technology for the treatment of crushed wood and agro-forestry residues [9,10], although tar formation is a problem to be solved prior to the use of syngas as a chemical raw material [11].

Both pyrolysis and gasification are technologies for producing biofuels, which are then stored, transported or used in subsequent transformation processes. Nevertheless, when energy (heat or electricity) is desired, the combustion of vegetable biomass has advantages concerning operating conditions and fuel flexibility [12,13].

Nowadays the two most developed technologies for obtaining heat and energy from biomass are grate and fluidized combustors [14,15]. The spouted bed is an alternative technology for solid fuel combustion, given that it has great advantages for the treatment of coarse and wide size distribution particles (as is the case of biomass) [16], and the turbulence of the regime ensures high heat and mass transfer rates [17], with pressure drop being much smaller than in fluidized beds [18,19].

The combustion efficiency and emission levels in vegetable biomass combustion systems depend on the properties of the fuel, operating conditions and combustor design [20]. Given that biomass is in many cases seasonal, the viability of any combustion plant requires adapting the operating conditions to the characteristics of the feed, and therefore biomass characterization should be fast, reliable and detailed. Accordingly, the aim of this paper is the development of a methodology based on a simple, fast and low cost analysis, such as TGA, to estimate all the usual analytical parameters required for a solid fuel characterization: elemental analysis, proximate analysis, heating value, and hemicellulose/cellulose/lignin ratio [21,22], which are the parameters of greater significance affecting degradation kinetics. DTG curve deconvolution is proposed for calculating the content of hemicellulose, cellulose and lignin [23,24] and the application of non-linear regression methods for correlating the contents of moisture, fixed carbon, volatile compounds and ashes with the contents of C, H, O and higher heating value, HHV [25–27].

2. Materials and methods

In order to study the different types of biomasses liable to energy recovery by combustion and with the aim of validating the methodology proposed with a sufficiently high number of materials, twelve types of biomasses have been used in this study, including commercial pellets, wood industry wastes (sawdust of *Pinus insignis, Acacia dealbata* and *Eucalyptus plantatio*), food industry wastes (rice husk, nut shells and olive stones), forest wastes (*Cytisus multiflorus, Pterospartum tridentatum* and *Pteridium aquilinum*) and two types of herbaceous materials (*Miscanthus sinensis* and *Rumex tianschanicus*). All these materials have been characterized in detail, with the physical–chemical properties measured being as follows: moisture content (according to ISO 589 standard and also in a HR83 halogen moisture analyzer, Mettler Toledo), proximate analysis (in a TA Instruments TGA Q5000IR following ASTM D5142 standard), elemental analysis (LECO TruSpec CHN analyzer and TruSpec-S module for S determination, according to ASTM D5373 and ISO19579 standards) and HHV (Parr 1356 isoperibolic bomb calorimeter following ASTM D5865 standard). The physical–chemical characteristics of the biomasses used in this study are shown in Table 1.

The moisture content of the materials used ranges from 7.21 wt.% w.b. (wet basis) for *Cytisus multiflorus* to 12.44 wt.% w.b. for *Pteridium aquilinum*, which are the usual equilibrium values for the conditions of temperature and moisture in the storeroom. These values significantly increase when the biomass is wet or when the atmospheric conditions are not favourable for collection. All the biomasses have high volatile matter contents, with values ranging from 65.33 wt.% dry basis (d.b.) for rice husk to 94.36 wt.% d.b. for *Cytisus multiflorus*. Concerning the other two parameters measured in the proximate analysis, Table 1 shows that vegetable biomass samples coming from different plant types or even from different parts of the plant have significantly different fixed carbon and ash contents. The content of fixed carbon is high in these biomass types derived from hard tissues (trunk, seeds), with values above 27 wt.% d.b. for olive stone, whereas in the case of soft tissues (leaves, young branches, bushes, grasses) the content is as low as 3.81 wt.% d.b. for *Rumex*. The ash content also changes significantly from sample to sample, with the values being even lower than 1 wt.% (pellet, nut shell, olive stone), whereas the values in the rice husk are close to 25 wt.% d.b. Carbon content ranges from 31.6 to 48.63 wt.% d.b., and N and S contents are generally low (around 1 wt.% d.b. or lower). The higher heating value (HHV) also varies considerably, with values ranging from 13.76 MJ kg^{-1} for rice husk to 20.36 MJ kg^{-1} for olive stone.

The methodology developed in this paper for fast characterization of the biomass is based on TGA, in the same equipment used for proximate analysis (TGA Q5000IR, TA Instruments). Accordingly, a detailed experimental study has been carried out in order

Table 1
Characterization of the vegetable biomasses studied.

Property	Pellet	*Pinus insignis*	*Acacia dealbata*	*Eucalyptus plantatio*	Rice husk	Nut shell	Olive stone	*Cytisus multiflorus*	*Pterospartum tridentatum*	*Pteridium aquilinum*	*Miscanthus sinensis*	*Rumex tianschanicus*
Moisture (wt.%. w.b.)	7.86	8.69	8.75	9.09	8.40	10.95	8.83	7.21	7.71	12.44	11.32	9.34
Volatile matter (wt.%. d.b.)	87.04	85.85	87.87	91.24	65.33	78.67	72.21	94.36	87.60	68.27	83.32	91.04
Fixed carbon (wt.%. d.b.)	12.25	12.79	9.64	6.95	10.04	21.08	27.21	4.17	10.68	22.09	12.27	3.81
Ashes (wt.%. d.b.)	0.71	1.35	2.50	1.81	24.63	0.25	0.58	1.46	1.71	9.63	4.41	5.14
C (wt.%. d.b.)	43.10	42.80	46.46	46.01	31.60	43.40	42.60	46.83	48.63	39.80	38.00	36.50
H (wt.%. d.b.)	6.25	6.42	4.86	4.35	5.20	6.40	6.46	4.87	5.15	6.06	6.21	5.88
N (wt.%. d.b.)	0.61	0.13	1.14	0.45	0.70	0.15	0.08	0.87	1.09	1.40	0.56	1.01
O (wt.%. d.b.)	49.31	49.28	44.99	47.37	37.79	49.79	50.26	45.91	43.37	42.73	50.55	51.28
S (wt.%. d.b.)	0.02	0.02	0.06	0.01	0.09	0.01	0.01	0.06	0.05	0.38	0.27	0.19
HHV (MJ kg^{-1})	18.74	18.84	17.10	18.87	13.76	20.12	20.36	17.30	18.50	17.50	18.26	16.91

w.b.: wet basis.
d.b.: dry basis.

to establish the optimum conditions for a reliable and reproducible determination of the contents of moisture, volatiles, fixed carbon and ash. Furthermore, a methodology based on the deconvolution of the DTG curve has been developed for clearly separating the peaks corresponding to the degradation of the three natural polymers contained in the biomass (hemicellulose, cellulose and lignin), and therefore determining their content. Accordingly, a specific algorithm written in Scilab has been developed, which uses the *ode* subroutine based on Adams method (for non-stiff ODE problems) for the integration of the ordinary differential equations describing the weight loss associated with the degradation of hemicellulose, cellulose and lignin (the kinetic model will be detailed below), and the *Fminsearch* subroutine (based on the algorithm by Nelder and Mead) for the optimization of the kinetic parameters of best fit to the experimental results. The correlations for predicting the elemental analysis and the HHV from the proximate analysis results have been obtained based on a Scilab algorithm using the *Leastsq* subroutine for linear and non-linear regression, i.e., the method of least squares. Fig. 1 shows the information flow diagram for the two algorithms developed.

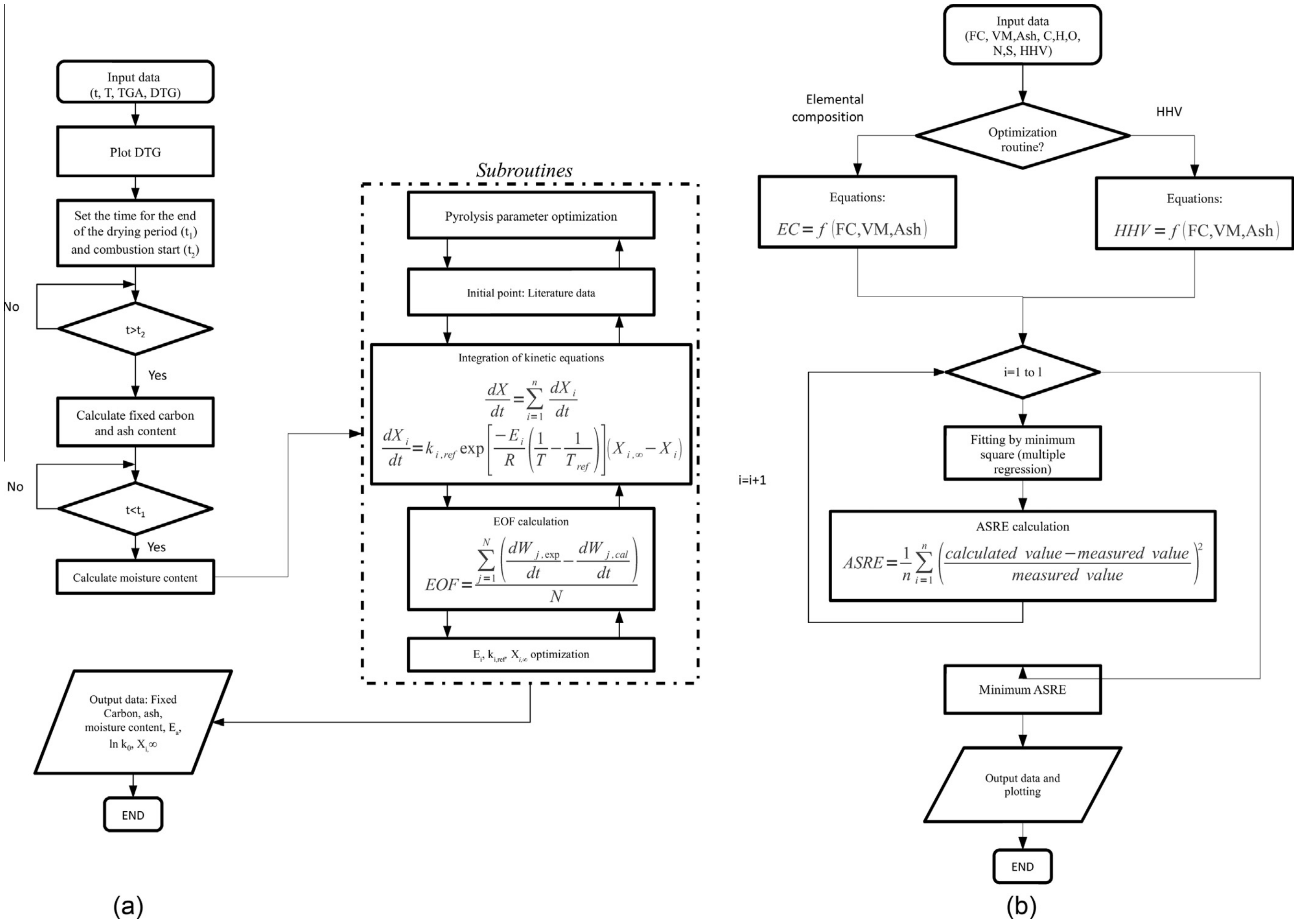
Input data (t, T, TGA, DTG)
Plot DTG
Set the time for the end of the drying period (t$_1$) and combustion start (t$_2$)
No
t>t$_2$
Yes
Calculate fixed carbon and ash content
No
t<t$_1$
Yes
Calculate moisture content
Subroutines
Pyrolysis parameter optimization
Initial point: Literature data
Integration of kinetic equations
$\frac{dX}{dt}=\sum_{i=1}^{n}\frac{dX_i}{dt}$
$\frac{dX_i}{dt}=k_{i,ref}\exp\left[\frac{-E_i}{R}\left(\frac{1}{T}-\frac{1}{T_{ref}}\right)\right](X_{i,\infty}-X_i)$
EOF calculation
$EOF=\frac{\sum_{j=1}^{N}\left(\frac{dW_{j,\exp}}{dt}-\frac{dW_{j,cal}}{dt}\right)}{N}$
E$_i$, k$_{i,ref}$, X$_{i,\infty}$ optimization
Output data: Fixed Carbon, ash, moisture content, E$_a$, ln k$_0$, X$_{i,\infty}$
END
(a)
Input data (FC, VM,Ash, C,H,O, N,S, HHV)
Elemental composition
Optimization routine?
HHV
Equations: $EC=f(\text{FC,VM,Ash})$
Equations: $HHV=f(\text{FC,VM,Ash})$
i=1 to I
i=i+1
Fitting by minimum square (multiple regression)
ASRE calculation
$ASRE=\frac{1}{n}\sum_{i=1}^{n}\left(\frac{calculated\ value-measured\ value}{measured\ value}\right)^2$
Minimum ASRE
Output data and plotting
END
(b)

Fig. 1. Flow charts of the algorithms designed for (a) DTG deconvolution and (b) determination of the experimental correlations relating proximate analysis, elemental analysis and HHV.

3. Results and discussion

3.1. Thermogravimetric analysis

A methodology has been developed for determining the content of each natural polymer making up the lignocellulosic biomass (hemicellulose, cellulose and lignin), which allows calculating in a single run the contents of moisture, volatiles, fixed carbon and ash, and provides a signal that is suitable for deconvolution. The setting up and tuning of this methodology required numerous assays by changing several operating parameters (type of gas and its flow rate, heating ramp, duration of isothermal periods). Mamleev et al. [28–30] reported that the thermal decomposition of cellulose is essentially the same in both air and nitrogen over a wide range of mass losses. Nevertheless, two different processes occur when oxidative atmospheres are used in thermobalance [24], one associated with the fast combustion of the volatiles produced by thermal degradation of hemicellulose and cellulose, and the other one associated with the combustion of the char. Therefore, the DTG signal obtained in the oxidative pyrolysis in thermobalance is not suitable for carrying out deconvolution, given that it does not provide the information pursued in this paper. Accordingly, an inert gas (He) was used with a flow rate of 60 mL min^{-1}, which allows a reliable measurement of polymer containing biomass degradation. The methodology tuned up consists in an isothermal period at 105 °C for 80 min to determine the moisture content by weight loss. Subsequently, the sample is heated to 700 °C following a 5 °C min^{-1} ramp, and kept at this temperature for 30 min. The weight loss during this period corresponds to the volatile matter. The inert gas is then substituted by air, with temperature and flow rate being the same for 5 min, which causes the combustion of the fixed carbon and allows the quantification of the unburnt ashes. Finally, the oven is cooled at a rate of 100 °C min^{-1} to room temperature. Fig. 2 outlines the methodology used.

The method designed for thermogravimetric analysis allows determining moisture content and the proximate analysis of the biomass without the need for additional assays, with the results being very similar to those obtained following the corresponding standard. Concerning moisture content, the results obtained with the methodology proposed are highly reproducible and accurate, i.e., the differences are lower than 5% with those obtained following standard procedures based on drying in an oven for long periods of time (ISO 589) or measuring in a halogen moisture analyser (HR83, Mettler Toledo). Likewise, the results obtained for volatile matter, fixed carbon and ash with the methodology developed are very similar to those obtained following ASTM D5142 standard method. It should be noted that the temperatures in the methodology proposed are lower than those in the standard method, given that the latter has specifically been designed for characterizing coals and cokes whose degradation temperatures are in all cases higher than those of biomass.

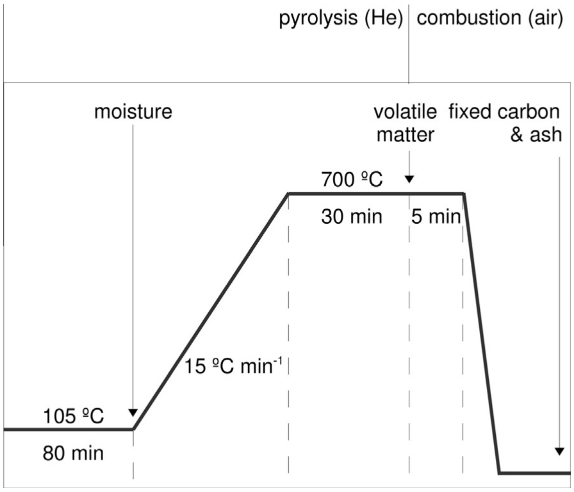

Fig. 2. Methodology developed for TGA.

Once moisture content has been determined and proximate analysis carried out, the values of DTG corresponding to the pyrolysis of the three natural polymers (without drying and combustion steps) are isolated by means of the algorithm designed. Subsequently, the deconvolution of the signal is approached according to a kinetic model considering three independent parallel reactions, without any interaction between them, corresponding to the decomposition of the three main biomass components: hemicellulose (HC), cellulose (C) and lignin (L) [31,32]. Accordingly, the overall kinetic equation is:

$$\left(\frac{1}{W_0 - W_\infty}\right)\left(\frac{dW}{dt}\right) = \sum_{i=1}^{n} c_i k_i \left[\frac{(W_i - W_{\infty,i})}{(W_{0,i} - W_{\infty,i})}\right]^{n_i} \qquad (1)$$

Biomass conversion, X, is defined as:

$$X = \frac{W_0 - W}{W_0 - W_\infty} \qquad (2)$$

where W_0 is the initial mass of the sample on a dry basis (at the end of the drying period), W_∞ the mass at the end of the pyrolysis step and W the mass at a given time. Similarly, the conversion of each constituent in the biomass is defined as:

$$X_i = \frac{W_{0,i} - W_i}{W_{0,i} - W_{\infty,i}} \qquad (3)$$

Several papers in the literature propose kinetic schemes for cellulose pyrolysis with a step for char formation [30,33]. Nevertheless, Chen and Kuo [34] reported that solid residue is hardly formed from the pyrolysis of individual hemicellulose and cellulose, but lignin pyrolysis is responsible for the formation of this material. In fact, it is well-known that the yield of char in the pyrolysis of biomass is directly related to the content of lignin [35], or even the phenol compounds derived from lignin in the pyrolysis of biomass may undergo repolymerization reactions at temperatures above 100 °C, giving way to a solid residue or secondary char, also called pyrolytic lignin [36,37]. Accordingly, the content of lignin may be calculated by summing the contribution of the deconvolution peak associated with lignin and the mass of char remaining at the end of the pyrolysis step (at the end of the isothermal period at 700 °C). Thus, whereas the masses of hemicellulose and cellulose at the end of the pyrolysis step ($W_{\infty,\mathrm{HC}}$ and $W_{\infty,\mathrm{C}}$ respectively) are zero, because these polymer are fully volatilized, the mass of lignin remaining in the particle ($W_{\infty,\mathrm{L}}$) is the mass of the sample minus the ash content.

Many authors propose a first order kinetics for the degradation of polymeric materials [38–41], whose overall kinetic equation is:

$$\frac{dX}{dt} = \sum_{i=1}^{n} \frac{dX_i}{dt} = \sum_{i=1}^{n} c_i k_i (X_{i,\infty} - X_i) \qquad (4)$$

where k_i is the kinetic constant corresponding to the degradation of each one of the three polymers. The kinetic constants are defined using the reparameterized Arrhenius equations, as follows:

$$k_i = k_{i,ref} \exp\left[\frac{-E_i}{R}\left(\frac{1}{T} - \frac{1}{T_{ref}}\right)\right] \qquad (5)$$

where $k_{i,ref}$ is the kinetic constant at the reference temperature T_{ref} (500 °C).

The kinetic parameters to be obtained by optimization are the kinetic constants at the reference temperature and the activation

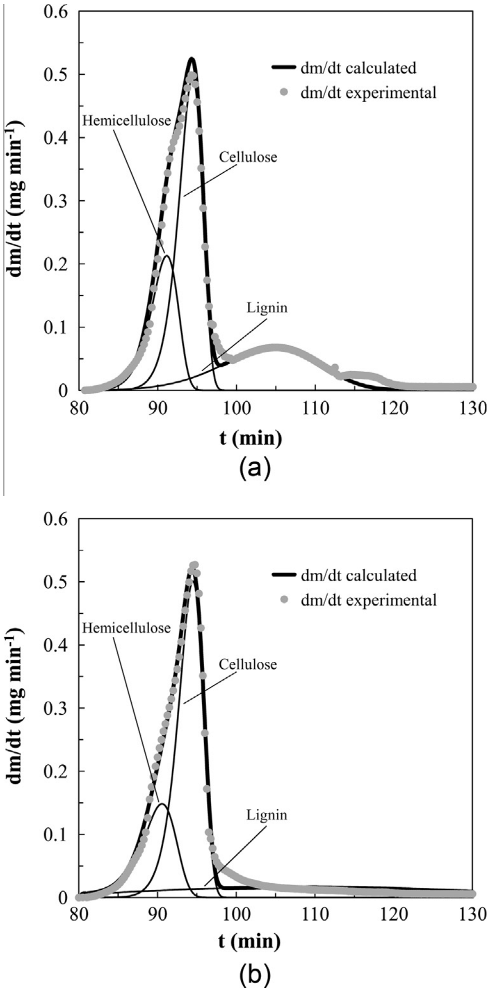

Fig. 3. Deconvolution of the DTG curve corresponding to the degradation of (a) rice husk and (b) *Cytisus multiflorus*.

energy for each one of the three parallel reactions, and the content of two of the three polymers (the third one is obtained by subtraction). The objective function to be optimized is defined as the sum of the squared differences between the experimental DTG data and those calculated by the model:

$$\mathrm{EOF} = \frac{\sum_{j=1}^{N}\left(\frac{dW_{j,exp}}{dt} - \frac{dW_{j,cal}}{dt}\right)^2}{N} \qquad (6)$$

where N is the number of experimental data. Fig. 3 shows as an example the deconvoluted DTG curve corresponding to two of the biomasses used in the study, namely, rice husk and *Cytisus multiflorus*.

In both the cases, hemicellulose is the least thermally stable of the wood components due to the presence of acetyl groups [42]. Lignin degradation starts at relatively low temperatures, proceeding over a wide range of temperatures [43]. Furthermore, Sebio-Puñal et al. [44] maintain that cellulose has higher thermal stability than both hemicellulose and lignin due to its crystalline structure, but in this study this is not always the case. Thus, in certain biomass types (*Pinus insignis*, *Miscanthus* or pellet) cellulose is the last polymer to begin its degradation, whereas in the remaining biomasses lignin begins its degradation at the same time or even later than cellulose. Once cellulose degradation has started, it is very fast and gives way to a characteristic sharp peak in the deconvoluted DTG curve. It is also observed that the tool designed for deconvolution performs well, given that it provides an excellent fitting between the experimental and calculated results. As mentioned above, this tool allows determining the kinetic parameters for the pyrolysis process (the kinetic constants at the reference temperature and so frequency factors and activation energies), as well as the content of each one of the natural polymers in the sample. The results obtained for the twelve samples selected are shown in Table 2.

Although there are no data in the literature for all the biomasses studied in this paper, certain results reported for pine sawdust and rice husk are going to be used for comparison purposes. Amutio et al. [24] pyrolized *Pinus insignis* sawdust and the values obtained for $\ln k_0$ (s^{-1}) and E (kJ mol^{-1}) are 11.2/133 (hemicellulose), 16.6/206 (cellulose) and 4.3/62 (lignin) for the pyrolyzable fractions of the three polymers. The values corresponding to polysaccharides (hemicellulose and cellulose) are similar to those obtained in this study (20.2/117 and 39.0/221 respectively). Higher differences are observed in the case of lignin, where the experimental data (−1.1/28.2) differ substantially, especially $\ln k_0$, which in fact becomes negative. This is attributed to the way of calculating lignin content. As previously stated, in this study lignin content is calculated by summing the contribution of the deconvolution peak associated with lignin and the mass of char remaining at the end of the pyrolysis step. This procedure is different from that applied by Amutio et al. [24]. Moreover, Teng et al. [45] pyrolysed rice husk and the values obtained are 27.5/154 (hemicellulose), 40.0/200 (cellulose) and 0.06/33. In a subsequent paper by Teng and Wei [46], the values reported are as follows: 9.8/154 (hemicellulose), 12.5/199 (cellulose) and −2.4/34 (lignin), which are also similar to the values obtained in this paper, with the highest differences corresponding to lignin. Therefore, the consistency between the results obtained and those reported in the literature validate the

Table 2
Contents of hemicellulose, cellulose and lignin (wt.%) and pyrolysis kinetic parameters for the 12 types of biomasses studied.

Biomass	Hemicellulose			Cellulose			Lignin		
	$\ln k_0$ (s^{-1})	E (kJ mol^{-1})	Content (wt.%)	$\ln k_0$ (s^{-1})	E (kJ mol^{-1})	Content (wt.%)	$\ln k_0$ (s^{-1})	E (kJ mol^{-1})	Content (wt.%)
Pellet	21.5	121.0	21.7	32.3	186.9	39.6	−5.0	11.3	34.5
Pinus insignis	20.2	117.4	21.9	39.0	221.5	35.7	−1.1	28.2	33.1
Acacia dealbata	23.7	119.9	8.5	12.8	86.8	62.6	−1.2	36.1	21.4
Eucalyptus plantatio	18.6	103.9	20.7	21.3	130.0	52.8	−4.0	21.8	21.5
Rice husk	16.0	94.2	15.0	21.5	129.3	30.8	1.3	45.8	26.4
Nut shell	19.1	107.8	21.1	25.7	153.5	39.1	1.0	39.8	32.2
Olive stone	20.3	108.4	10.1	21.8	118.8	22.0	30.2	172.9	60.8
Cytisus multiflorus	11.6	73.8	19.6	20.2	123.1	50.6	-6.1	10.0	25.8
Pterospartum tridentatum	9.5	63.5	23.7	19.5	120.7	37.4	1.5	43.1	33.6
Pteridium aquilinum	13.2	76.2	9.7	15.0	94.8	31.2	−0.1	34.4	42.1
Miscanthus sinensis	14.4	85.0	24.7	17.7	111.1	38.5	−5.1	17.8	24.6
Rumex tianschanicus	14.3	77.8	11.3	13.0	84.6	42.6	−1.7	33.5	36.0

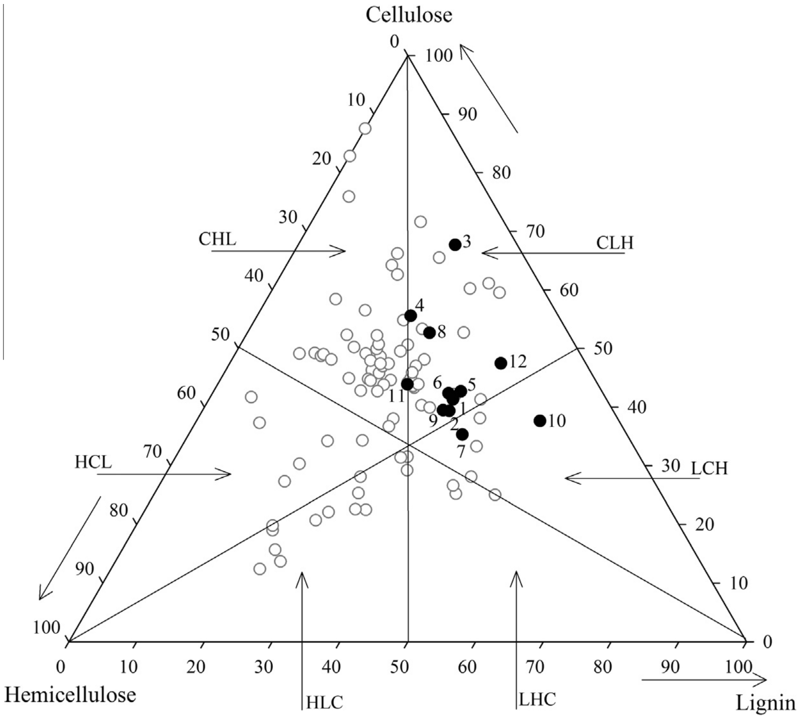

Fig. 4. Structural composition of the different biomass varieties on a ternary diagram. (●) Biomasses in this paper: 1. Pellet, 2. *Pinus insignis*, 3. *Acacia dealbata*, 4. *Eucalyptus plantation*, 5. Rice husk, 6. Nut shell, 7. Olive pit, 8. *Cytisus multiflorus*, 9. *Pterospartum tridentatum*, 10. *Pteridium aquilium*, 11. *Miscanthus sinensis*, and 12. *Rumex tianschanicus*. (○) Data gathered by Vassilev et al. [22].

methodology proposed for analysing the experimental data. Table 2 shows that cellulose is generally the component with the highest activation energy, with values ranging from 84.6 to 221.5 kJ mol^{-1} for eucalyptus sawdust and pine sawdust, respectively, and the lowest activation energy corresponds to lignin, given that in all cases it was lower than those for the other two components of the biomass. The same happens with the values of $\ln k_0$, which are very low or even negative in many cases. Concerning the content of each one of the natural polymers making up the biomass, Vassilev et al. [22] have proven that the proportions of structural components in different biomass varieties are highly variable. Following the classification methodology proposed by these authors, Fig. 4 shows that most of the biomasses studied in this paper belong to CLH group (cellulose content > lignin content > hemicellulose content), except *Miscanthus sinensis*, which is CHL type, and both *Pteridium aquilinum* and olive pit belong to LCH group. The values collected by Vassilev et al. [22] have also been included in Fig. 4.

3.2. Empirical correlations

Empirical correlations have been determined for predicting the HHV and the elemental composition (EC) from the values obtained in the proximate analysis, which is much simpler, faster and cheaper to carry out than the standard procedures for determining HHV and EC. Furthermore, techniques based on the generalized method of least squares have been used to fit the experimental data to the algebraic expressions proposed by Parikh et al. [26] for HHV and Parikh et al. [27] for EC, Table 3. The validity has also been analysed for the correlations with the coefficients proposed by these authors.

Average square relative error (ASRE) was defined as the objective function to be minimized. According to this definition, ASRE is closely related to the regression or determination coefficient:

Table 3
Correlations used for data fitting.

Proposed expression	Eqs.
$\mathrm{HHV} = a\mathrm{FC} + b\mathrm{VM} + c\mathrm{A}$	(8)
$\mathrm{HHV} = a\mathrm{FC} + b\frac{\mathrm{FC}}{\mathrm{VM}} + c\mathrm{VM} + d\mathrm{A}$	(9)
$\mathrm{HHV} = \mathrm{AFC} + b\mathrm{FC}^2 + c\mathrm{FCVM} + d\mathrm{VM} + e\mathrm{VM}^2 + f\mathrm{A}$	(10)
$\mathrm{HHV} = a\mathrm{FC} + b\mathrm{VM}$	(11)
$\mathrm{HHV} = a\mathrm{FC} + b\mathrm{VM}^c$	(12)
$\mathrm{HHV} = a\mathrm{FC}^b + c\mathrm{VM}^d$	(13)
$\mathrm{HHV} = a\mathrm{FC}^b + c\mathrm{VM}$	(14)
$\mathrm{HHV} = a\mathrm{FC} + b\mathrm{VM}^c + d\mathrm{A}$	(15)
$\mathrm{HHV} = a + b(\mathrm{FC} + \mathrm{VM}) + c\mathrm{A}$	(16)
$\mathrm{EC} = a\mathrm{FC} + b\frac{\mathrm{FC}}{\mathrm{VM}} + c\mathrm{VM}$	(17)
$\mathrm{EC} = a\mathrm{FC} + b\mathrm{FC}^2 + c\mathrm{FCVM} + d\mathrm{VM} + e\mathrm{VM}^2$	(18)
$\mathrm{EC} = a\mathrm{FC} + b\mathrm{VM}$	(19)
$\mathrm{EC} = a\mathrm{FC} + b\mathrm{VM}^c$	(20)
$\mathrm{EC} = a\mathrm{FC}^b + c\mathrm{VM}^d$	(21)
$\mathrm{EC} = a\mathrm{FC}^b + c\mathrm{VM}$	(22)
$\mathrm{EC} = \mathrm{FC} + a\mathrm{VM}$	(23)

Table 4
Equations of best fit and their parameters and ASRE values.

Eq.	HHV (MJ kg^{-1})	EC (wt.% d.b.)		
		C	H	O
	(9)		(18)	
a	0.6030	3.164	−0.6601	−1.7740
b	−22.56	$-4.645 \cdot 10^{-2}$	$1.256 \cdot 10^{-3}$	$4.144 \cdot 10^{-2}$
c	0.1705	$-1.099 \cdot 10^{-2}$	$8.143 \cdot 10^{-3}$	$6.669 \cdot 10^{-3}$
d	$-7.877 \cdot 10^{-4}$	0.2786	0.2343	1.105
e	–	$6.811 \cdot 10^{-3}$	$-2.031 \cdot 10^{-3}$	$-5.673 \cdot 10^{-3}$
ASRE	$2.35 \cdot 10^{-3}$	$3.44 \cdot 10^{-3}$	$8.72 \cdot 10^{-3}$	$3.63 \cdot 10^{-3}$

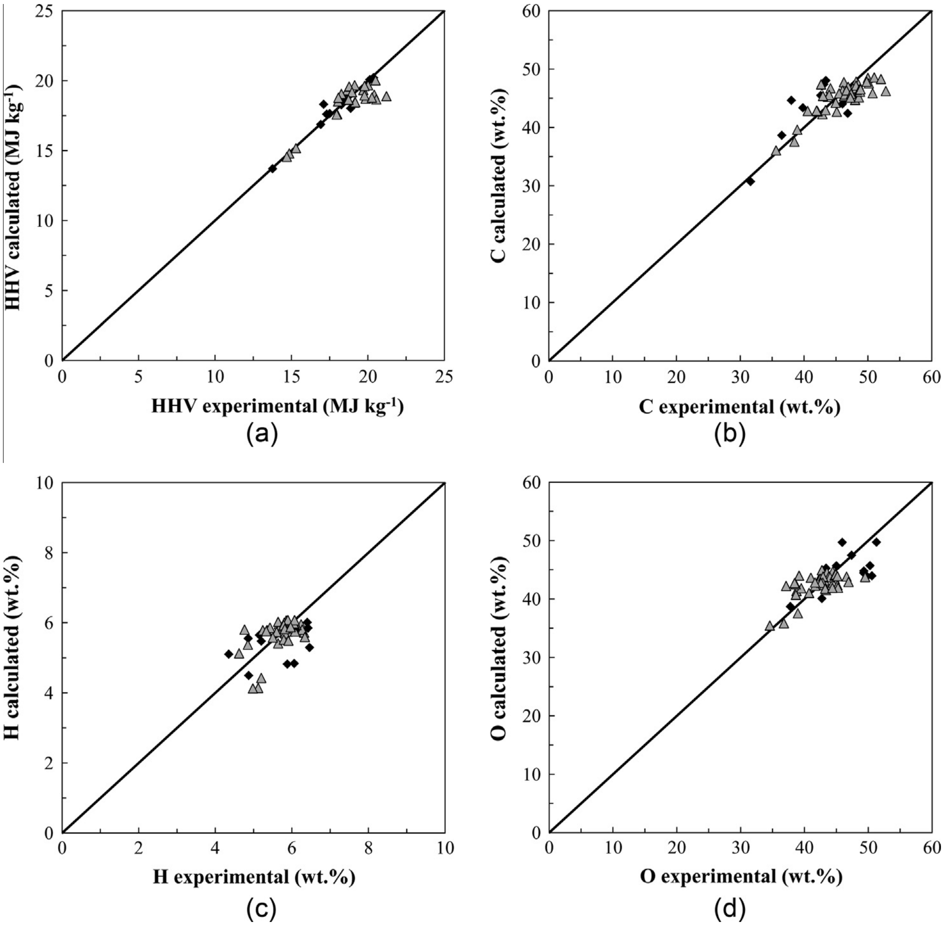

Fig. 5. Comparison of the experimental values with the calculated ones. (a) HHV, (b) C, (c) H, and (d) O. (●) This paper. (●) Data gathered by Channiwala and Parikh [25], Vassilev et al. [21] and Link et al. [47].

$$\mathrm{ASRE} = \frac{1}{n}\sum_{i=1}^{n}\left(\frac{\text{calculated value} - \text{measured value}}{\text{measured value}}\right)^2 \quad (7)$$

As observed in Table 3, the equations used in the fitting are those for calculating HHV and EC. Some of them are linear combinations of fixed carbon (FC) and volatile matter (VM) (Eqs. (11), (19) and (23)), or even ash content (A) and/or FC/VM ratio (Eqs. (8), (9), (16) and (17), and others are polynomial equations (Eqs. (10) and (18)) or non-linear variable combinations (Eqs. (12)–(15), (20)–(22)).

In addition to the data corresponding to the twelve biomass varieties used in this study, data obtained by other authors [21,25,47] have also been used in the fitting, which involves a wider range of experimental data and validity of the correlations proposed. The equations of best fit, the optimum values of the parameters and their corresponding ASRE values are shown in Table 4. Fig. 5 shows the adequacy of the fitting between the experimental and calculated data.

The most suitable equation for calculating HHV is Eq. (9). Although Eq. (10) reduces the ASRE by 0.4%, this improvement is not significant and does not justify the use of an extra fitting parameter. Eq. (9) is a linear combination of four parameters obtained in the proximate analysis, as are: FC, VM, A and the FC/VM ratio. This equation contains more parameters than other equations proposed in the literature [26,48], which is reflected in the excellent fitting observed in Fig. 5a for the 40 types of biomasses used and the lower sum of square errors than any other correlation in the literature. Thus, ASRE is 140% higher for the equation proposed by Cordero et al. [48], which predicts HHV by means of a linear combination of FC and VM, and 108% higher for the equation proposed by Parikh et al. [26], which also includes a linear relationship of HHV with A.

The equation that provides best results for the elemental composition is Eq. (18), which has 5 fitting parameters and is a second order polynomial equation whose variables are the contents of major elements (C, H, O) and two parameters obtained by proximate analysis, i.e., FC and VM. Although the equation proposed involves the use of three parameters more than the one proposed by Parikh et al. [27], there is a significant reduction in the sum of square errors, and as observed in Fig. 5 the fitting between the experimental and calculated values is excellent. Thus, the parameters of best fit proposed by Parikh et al. [27] have been used for the estimation of the ultimate analysis corresponding to the 54 types of biomasses used in this study, and the ASRE values obtained are significantly higher: 30.8% for oxygen, 68.1% for carbon and as high as 200% for hydrogen content. Furthermore, none of the correlations proposed allow predicting the content of N and S, given that although C, H and O are directly related to volatile matter and fixed carbon, the content of N and S depends on the type of tissue and biomass variety.

4. Conclusions

A methodology has been developed for biomass characterization, which is based on thermogravimetric analysis, deconvolution of the DTG signal and the use of empirical correlations obtained in this study. The methodology allows accurately determining the results that are commonly determined by using the corresponding standard methods, which require specific equipment and much more sophisticated and expensive analytical procedures. The TGA includes a 80 min drying step, pyrolysis in an inert atmosphere at 700 °C and a combustion step, which allow calculating the moisture content and the proximate analysis. The deconvolution of the DTG signal allows calculating the content of each one of the natural polymers, as well as the parameters describing the thermal degradation of the biomass, which are essential for ascertaining combustion time in any industrial unit. A regression analysis by least squares of the different correlations proposed in literature has driven to the proposal of faithful correlations for accurately determining HHV and elemental analysis (C, H and O), which are essential parameters that condition thermal balance in any combustion process.

Acknowledgements

This work was carried out with the financial support from the Ministry of Science and Education of the Spanish Government (Project CTQ2010-16133), the FEDER Funds (European Union), the Basque Government (Project IT748-13) and the University of the Basque Country UPV/EHU (UFI 11/39). Juan Saldarriaga is grateful for the Ph.D. grant from the Administrative Department of Science, Technology and Innovation, COLCIENCIAS (Colombia). Aitor Pablos is grateful for the Ph.D. grant from the University of the Basque Country.

References

[1] Ragauskas AJ, Williams CK, Davison BH, Britovsek G, Cairney J, Eckert CA, et al. The path forward for biofuels and biomaterials. Science 2006;311:484–9.
[2] Frombo F, Minciardi R, Robba M, Rosso F, Sacile R. Planning woody biomass logistics for energy production: a strategic decision model. Biomass Bioenergy 2009;33:372–83.
[3] Luque R, Herrero-Davila L, Campelo JM, Clark JH, Hidalgo JM, Luna D, et al. Biofuels: a technological perspective. Energy Environ Sci 2008;1:542–64.
[4] Fernandez RG, Garcia CP, Lavin AG, Bueno de las Heras J. Study of main combustion characteristics for biomass fuels used in boilers. Fuel Process Technol 2012;103:16–26.
[5] Wright MM, Daugaard DE, Satrio JA, Brown RC. Techno-economic analysis of biomass fast pyrolysis to transportation fuels. Fuel 2010;89:S2–S10.
[6] Aguado R, Olazar M, San J, Aguirre G, Bilbao J. Pyrolysis of sawdust in a conical spouted bed reactor. Yields and product composition. Ind Eng Chem Res 2000;39:1925–33.
[7] Mohan D, Charles U, Steele PH. Pyrolysis of wood/biomass for bio-oil: a critical review. Energy Fuels 2006;20:848–89.
[8] Valle B, Castaño P, Olazar M, Bilbao J, Gayubo AG. Deactivating species in the transformation of crude bio-oil with methanol into hydrocarbons on a HZSM-5 catalyst. J Catal 2012;285:304–14.
[9] Yin R, Liu R, Wu J, Wu X, Sun C, Wu C. Influence of particle size on performance of a pilot-scale fixed-bed gasification system. Bioresour Technol 2012;119:15–21.
[10] Erkiaga A, Lopez G, Amutio M, Bilbao J, Olazar M. Influence of operating conditions on the steam gasification of biomass in a conical spouted bed reactor. Chem Eng J 2014;237:259–67.
[11] Gomez-Barea A, Ollero P, Leckner B. Optimization of char and tar conversion in fluidized bed biomass gasifiers. Fuel 2013;103:42–52.
[12] Koornneef J, Junginger M, Faaij A. Development of fluidized bed combustion: an overview of trends, performance and cost. Prog Energy Combust Sci 2007;33:19–55.
[13] Khan AA, de Jong W, Jansens PJ, Spliethoff H. Biomass combustion in fluidized bed boilers: potential problems and remedies. Fuel Process Technol 2009;90:21–50.
[14] Sirisomboon K, Kuprianov VI, Arromdee P. Effects of design features on combustion efficiency and emission performance of a biomass-fuelled fluidized-bed combustor. Chem Eng Process Process Intensif 2010;49:270–7.
[15] Tarelho LAC, Neves DSF, Matos MAA. Forest biomass waste combustion in a pilot-scale bubbling fluidised bed combustor. Biomass Bioenergy 2011;35:1511–23.
[16] Altzibar H, Lopez G, Aguado R, Alvarez S, San Jose MJ, Olazar M. Hydrodynamics of conical spouted beds using different types of internal devices. Chem Eng Technol 2009;32:463–9.
[17] Makibar J, Fernandez-Akarregi AR, Alava I, Cueva F, Lopez G, Olazar M. Investigations on heat transfer and hydrodynamics under pyrolysis conditions of a pilot-plant draft tube conical spouted bed reactor. Chem Eng Process Process Intensif 2011;50:790–8.
[18] Olazar M, San Jose MJ, Peñas FJ, Aguayo AT, Bilbao J. Stability and hydrodynamics of conical spouted beds with binary mixtures. Ind Eng Chem Res 1993;32:2826–34.
[19] Olazar M, San Jose MJ, Lamosas R, Bilbao J. Hydrodynamics of sawdust and mixtures of wood residues in conical spouted beds. Ind Eng Chem Res 1994;33:993–1000.
[20] Janvijitsakul K, Kuprianov VI. Similarity and modeling of axial CO and NO concentration profiles in a fluidized-bed combustor (co-)firing biomass fuels. Fuel 2008;87:1574–84.
[21] Vassilev SV, Baxter D, Andersen LK, Vassileva CG. An overview of the chemical composition of biomass. Fuel 2010;89:913–33.
[22] Vassilev SV, Baxter D, Andersen LK, Vassileva CG, Morgan TJ. An overview of the organic and inorganic phase composition of biomass. Fuel 2012;94:1–33.
[23] Conesa JA, Domene A. Biomasses pyrolysis and combustion kinetics through n-th order parallel reactions. Thermochim Acta 2011;523:176–81.
[24] Amutio M, Lopez G, Aguado R, Artetxe M, Bilbao J, Olazar M. Kinetic study of lignocellulosic biomass oxidative pyrolysis. Fuel 2012;95:305–11.
[25] Channiwala SA, Parikh PP. A unified correlation for estimating HHV of solid, liquid and gaseous fuels. Fuel 2002;81:1051–63.
[26] Parikh J, Channiwala SA, Ghosal GK. A correlation for calculating HHV from proximate analysis of solid fuels. Fuel 2005;84:487–94.
[27] Parikh J, Channiwala SA, Ghosal GK. A correlation for calculating elemental composition from proximate analysis of biomass materials. Fuel 2007;86:1710–9.
[28] Mamleev V, Bourbigot S, Yvon J. Kinetic analysis of the thermal decomposition of cellulose: the change of the rate limitation. J Anal Appl Pyrolysis 2007;80:141–50.
[29] Mamleev V, Bourbigot S, Yvon J. Kinetic analysis of the thermal decomposition of cellulose: the main step of mass loss. J Anal Appl Pyrolysis 2007;80:151–65.
[30] Mamleev V, Bourbigot S, Le Bras M, Yvon J. The facts and hypotheses relating to the phenomenological model of cellulose pyrolysis: interdependence of the steps. J Anal Appl Pyrolysis 2009;84:1–17.
[31] Caballero JA, Conesa JA. Mathematical considerations for nonisothermal kinetics in thermal decomposition. J Anal Appl Pyrolysis 2005;73:85–100.
[32] Varhegyi G. Aims and methods in non-isothermal reaction kinetics. J Anal Appl Pyrolysis 2007;79:278–88.
[33] Lin YC, Cho J, Tompsett GA, Westmoreland PR, Huber GW. Kinetics and mechanism of cellulose pyrolysis. J Phys Chem C 2009;113:20097–107.
[34] Chen WH, Kuo PC. Isothermal torrefaction kinetics of hemicellulose, cellulose, lignin and xylan using thermogravimetric analysis. Energy 2011;36:6451–60.
[35] Di Blasi C. Modeling chemical and physical processes of wood and biomass pyrolysis. Prog Energy Combust Sci 2008;34:47–90.
[36] Hosoya T, Kawamoto H, Saka S. Pyrolysis behaviors of wood and its constituent polymers at gasification temperature. J Anal Appl Pyrolysis 2007;78:328–36.
[37] Gayubo AG, Valle B, Aguayo AT, Olazar M, Bilbao J. Pyrolytic lignin removal for the valorization of biomass pyrolysis crude bio-oil by catalytic transformation. J Chem Technol Biotechnol 2010;85:132–44.
[38] Lopez G, Aguado R, Olazar M, Arabiourrutia M, Bilbao J. Kinetics of scrap tyre pyrolysis under vacuum conditions. Waste Manage 2009;29:2649–55.
[39] Castro A, Soares D, Vilarinho C, Castro F. Kinetics of thermal de-chlorination of PVC under pyrolytic conditions. Waste Manage 2012;32:847–51.
[40] Ding F, Xiong L, Luo C, Zhang H, Chen X. Kinetic study of low-temperature conversion of plastic mixtures to value added products. J Anal Appl Pyrolysis 2012;94:83–90.
[41] Hayhurst AN. The kinetics of the pyrolysis or devolatilisation of sewage sludge and other solid fuels. Combust Flame 2013;160:138–44.
[42] Yang H, Yan R, Chen H, Lee DH, Zheng C. Characteristics of hemicellulose, cellulose and lignin pyrolysis. Fuel 2007;86:1781–8.
[43] Yang H, Yan R, Chen H, Zheng C, Lee DH, Liang DT. In-depth investigation of biomass pyrolysis based on three major components: hemicellulose, cellulose and lignin. Energy Fuel 2005;20:388–93.
[44] Sebio-Puñal T, Naya S, Lopez-Beceiro J, Tarrio-Saavedra J, Artiaga R. Thermogravimetric analysis of wood, holocellulose, and lignin from five wood species. J Therm Anal Calorim 2012;109:1163–7.
[45] Teng H, Lin HC, Ho JA. Thermogravimetric analysis on global mass loss kinetics of rice hull pyrolysis. Ind Eng Chem Res 1997;36:3974–7.
[46] Teng H, Wei YC. Thermogravimetric studies on the kinetics of rice hull pyrolysis and the influence of water treatment. Ind Eng Chem Res 1998;37:3806–11.
[47] Link S, Arvelakis S, Paist A, Martin A, Liliedahl T, Sjöström K. Atmospheric fluidized bed gasification of untreated and leached olive residue, and co-gasification of olive residue, reed, pine pellets and Douglas fir wood chips. Appl Energy 2012;94:89–97.
[48] Cordero T, Marquez F, Rodriguez-Mirasol J, Rodriguez JJ. Predicting heating values of lignocellulosics and carbonaceous materials from proximate analysis. Fuel 2001;80:1567–71.